Study on Preparation and First-Stage Sintering Kinetics of ThO₂-UO₂ Pellets Made by Sol-Gel Microspheres Technique

A.S. Sökücü[a,*], M. Bedir[b], M.T. Aybers[a]

[a]Çekmece Nuclear Research and Training Center, 34303, Istanbul, Turkey
[b]Department of Physics Engineering, University of Gaziantep, 27310, Gaziantep, Turkey

The sol-gel method, which is among the methods used for the production of ThO₂-UO₂ mixed oxide fuel pellets, allows a high degree of micro-homogeneity of uranium and thorium in the solution stage. The present study seeks to develop an alternative method in order to produce mixed thorium-uranium dioxide fuel pellets, prepared by internal gelation technique of sol-gel process. The study also aims to investigate shrinkage behavior and first-stage sintering kinetics of pellets compacted in the Ar-5%H₂ atmosphere using a dilatometer. The chemical and physical properties such as density, homogeneity, O/M ratio, metallic impurities, unit cell parameters, phase contents and surface area of powders, that have different compositions of thoria-urania, were studied. The influences of sintering parameters on the characteristics of microspheres and on the properties of sintered pellets are discussed.

1. Introduction

The internal gelation process (IGP) is one of the most important routes of the sol-gel process to prepare $(Th,U)O_2$ gel microspheres. $(Th,U)O_2$ mixed oxide fuel contains daughter products of ^{232}U, namely ^{212}Bi and ^{208}Tl, which emit strong gamma radiations of 1.8 MeV and 2.6 MeV respectively. They are hazardous to human health. In addition, it is more difficult to get a homogeneous mixture of two different powders by powder metallurgical method. Sol-gel process is thus an alternative fabrication process to reduce the radiation dose received by the operators, offering a great degree of pellet homogeneity [1, 2]. Homogeneous composition simplifies the solid solution formation of mixed oxides which is an important prerequisite to obtain good pellets in the sintering step of the process [3–5].

Sintering is a key step in most of the processes which deal with the elaboration of ceramic materials. It is a complicated process that contains micro-structural evolution by densification through several different transport mechanisms. The main factors which influence the sintering are temperature, annealing time, green density, and bulk composition [6, 7].

Materials with high melting point, such as nuclear ceramics, require high sintering temperatures. The design of sintering cycles, that minimizes the energy consumption, while attaining a certain target density and uniform microstructure, is of great use. Minimizing of sintering time reduces grain growth, providing a better sintered strength and other physical properties [8].

The sintering process is a diffusion controlled process, the rate of which is controlled by more slowly moving metal atoms [9, 10]. Determination of the basic physical mechanisms of sintering for a given material system is important for the kinetic mechanisms by which densification and grain growth occur during sintering. The mechanisms of material movement in sintering are not only important in determining the properties of the end product but also have fascinated the powder technologists since they started to contend with the science of sintering. Therefore, it is very important to study the kinetic parameters of sintering accurately [11].

Several methods have been reported in the literature for the calculation of the kinetic parameters from a series of sintering curves, obtained at different linear-heating rates. The Arrhenius plots of the shrinkage rate at equal values of the shrinkage have been commonly used to estimate the activation energy of the initial stage of sintering.

Considerable amount of works have been reported on sintering and sintering kinetics of UO_2 and ThO_2 in the literature. Although the initial stage of the sintering of UO_2 and ThO_2 alone has been investigated in detail, not much work has been reported on sintering kinetics of mixed oxides $(Th,U)O_2$ [11–15].

The study determined the activation energy for sintering using the dilatometric technique. Therefore, dilatometric runs were performed in ThO₂-5%UO₂, ThO₂-10%UO₂ (composition in wt.%) compacts in Ar-5%H₂ with heating rates of 5 °C/min, the output of which was used to generate the activation energy for sintering.

2. Theory of sintering

The activation energy, Q, in the initial stage of sintering was estimated by graphical method of isothermal shrinkage of pellets. The detailed discussion of the method and the major steps for calculation of Q are given in the following paragraphs.

Various methods have been used to study the sintering mechanism, among which are dilatometric studies

of the kinetics of isothermal shrinkage of powder compacts, which are particularly useful because they allow one to contiguously follow dimensional variation in the same sample.

The experimental shrinkage curves generally follow an equation of the form

$$\Delta L/L_0 = Y = [K(T)t]^n, \tag{1}$$

where

$$K(T) = A\gamma\Omega D/kTr^3. \tag{2}$$

In this equation L_0 is the initial sample length at the beginning of sintering, $K(T)$ Arrhenius constant, D the diffusion coefficient (cm^2/s), r the particle radius (cm), γ the surface tension (erg/cm^2), Ω the vacancy volume (cm^3), A, n are the constants which values depend on the sintering mechanism and k the Boltzmann constant.

It is very difficult to determine the origin of the curve since the sample would not reach the isothermal temperature immediately. Following the time and shrinkage correction Eq. 1 became [16]:

$$Y + Y_0 = K^n(t + t_0)^n (t_0 << 0) \tag{3}$$

Differentiation form of the equation gives the following:

$$dY/dt = Y' = nK^n t^{n-1} \tag{4}$$

Y' can be calculated from experimental data. By plotting $\log Y'$ versus $\log t$ a straight line (slope: $n - 1$) will be obtained for each isothermal temperature (Fig. 4). The value of n (determination of sintering mechanism) can be determined from the slope of this line and $K(T)$ from the intercept with the $\log Y'$ axis. When $K(T)$ is known, the diffusion coefficient can be calculated from Eq. 2.

For the variation of $\log D$ versus $1/T$, the expression is as follows

$$D = D_0 \exp(-Q/RT), \tag{5}$$

where D_0 is the preexponential factor of Arrhenius equation, Q the activation energy and R the molar gas constant.

The apparent activation energy is calculated from the slope of the variation of $\ln D$ versus $1/T$ (a straight line). The slope of the plot of $\ln D$ vs. $1/T$ gives the $-Q/R$. R being a constant with value of $8.31441 \, \mathrm{J\,K^{-1}\,mol^{-1}}$, Q is determined from the slope of the plot (Fig. 5).

3. Experimental procedure

The initial materials are uranyl nitrate hexahydrate (UNH) and commercial thorium nitrate. Uranyl nitrate hexahydrate (UNH) was prepared by the conversion of U_3O_8, which was supplied by Canada Atomic Energy, to the ammonium diuranate or (ADU) form at Çekmece Research and Training Center. The commercial thorium nitrate salt supplied by company of Rhone-Poulench. The metallic impurity contents of uranyl nitrate and thorium nitrate salts are smaller than 700 ppm.

The ThO_2-5%UO_2 and ThO_2-10%UO_2 green pellets for this study were prepared by the internal gelation process, in which we used the solutions of desired mixtures of the uranium and thorium nitrates. The feed-broth was prepared by mixing the cooled metal nitrate solution with the cooled mixture of hexamethylenetetramine (HMTA) and urea. The feed-broth was dispersed as droplets into a gelation column containing the hot silicone oil. The formed gel microspheres were separated from the oil and were first washed with carbon tetrachloride to remove the adhered silicon oil, followed by washing with ammonium hydroxide, to remove the ammonium nitrate as well as the unreacted HMTA and urea. Washed microspheres were dried at 100 °C, calcined at around 700 °C for five hours to remove the residual organic, and reduced in Ar+5%H_2 gas mixture at 650 °C for 1.5 hours. The reduced microspheres were crushed to characterize the starting materials before sintering steps.

The flow-sheet used for the preparation of ThO_2-5%UO_2 and ThO_2-10%UO_2 pellets by internal gelation in the present study is shown in Fig. 1.
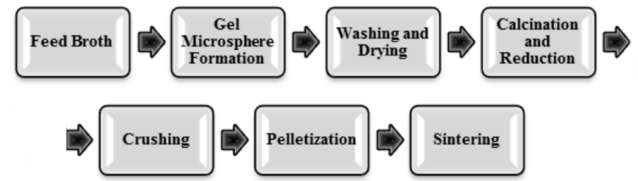

Fig. 1. Flow sheet for the preparation of ThO_2-5%UO_2 and ThO_2-10%UO_2 pellets by internal gelation.

In order to evaluate the influence of the preparation method on several chemical compositions of the powders as well as the sintered pellets, the microstructural characterization of the powdered compounds was undertaken in terms of thermogravimetry (TGA/DTA), specific surface area (BET) and crystallization state (XRD). The X-ray diffraction data of powders confirm that the compounds are face centered cubic (FCC) and single phased before the sintering.

The TGA/DTA curves for ThO_2-5%UO_2 and ThO_2-10%UO_2 powders oxidation were measured by TGA/DTA-Netzsch STA 449 C simultaneous thermal analyzer up to 800 °C at 10 °C/min in air atmosphere. Samples were cooled down to room temperature when the desired temperature was reached. The powders were placed in platinum covered crucibles, an empty crucible being the reference. Oxygen-metal ratios (O/M) of the powders were calculated by thermogravimetric analysis.

Before sintering procedures, the specific surface area of the ThO_2-5%UO_2 and ThO_2-10%UO_2 precursor powders were measured using the BET method with nitrogen as the adsorbate gas. N_2 adsorption and desorption isotherms were measured by Quantachrome Autosorb System at different temperatures. All samples were first degassed in a vacuum at high temperatures. The adsorption and desorption BET isotherms of the ThO_2-5%UO_2 and ThO_2-10%UO_2 powders were prepared by heating to 150 °C and ThO_2 powder were prepared by heating to 300 °C.

The phase analysis was performed using X-ray diffractometry (Bruker AXS D8 Advance diffractometer). The

crystallite sizes were evaluated by step scanning diffraction X-ray profile employing a Siemens ceramic X-ray equipped with a CuK_α tube for diffractometry, operated at 40 kV and 40 mA. The crystallite size was determined from the line broadening of XRD peaks; the full scan of 2θ range from 20° to 80° was carried at low speed of 0.01 °/min. The Philips software allows the crystallite size determination through the comparison of profile lines broadening related to a standard material, for which purpose Scherrer's relation was used [17].

The characterizations of the powders are performed considering the specification. The relevant data used in further calculation of activation energy are shown in Table I. After the characterization process, powders are compacted into green pellets of 6 mm diameter and around 4 mm in height. The green density of the pellets has been calculated by geometrical method.

Characteristics of starting ThO_2-5%UO_2 and ThO_2-10%UO_2 powders.   TABLE I

Property	ThO_2-5%UO_2	ThO_2-10%UO_2
Theoretical density, ρ [g/cm^3]	10.048	10.096
O/M ratio	2.254	2.167
Surface energy, γ [erg/cm^2]	1122.5	1095
Specific surface area, S [m^2/g]	3.0741	2.5016
Particle radius, a[A]	5.59	5.94
Metallic impurities, [ppm]	< 1000	< 1000

The sintering behavior of the ThO_2-5%UO_2 and ThO_2-10%UO_2 pellets prepared by internal gelation process was studied by measuring the shrinkage in axial direction using a push rod type dilatometer (Netzsch DIL 402 C). The length change measurements were made by Linear Voltage Differential Transformer (LVDT), which was maintained at a constant temperature by means of water circulation from a constant temperature bath. The accuracy of the measurement of change in length was within $\pm 0.1\ \mu$m. The temperature was measured using a calibrated Pt/Pt Rh10% thermocouple which was placed closely above the sample. A small force of 0.25 N was applied to the sample through the push rod.

The dilatometric experiments were carried out in the temperature range of 100–1200 °C in reducing Ar+5%H_2 atmosphere, at a heating rate of 5 °C/min. The shrinkage of the standard sample was measured under the same condition to correct the differences in shrinkage between in the sample holder and the sample. The selection of the temperature programme was made by computer via the data acquisition system. The dilatometric data which were obtained are in the form of curves of dimension against time and temperature. Time vs. dimensional shrinkage plots were obtained from dilatometric studies for all the pellets. The data obtained were thus analyzed to find out the kinetics of sintering and the activation energies of the ThO_2-5%UO_2 and ThO_2-10%UO_2 pellets.

4. Experimental results

Figure 2 shows the shrinkage behaviors of ThO_2-5%UO_2 and ThO_2-10%UO_2 pellets under Ar+5%H_2 atmosphere. The dL/L values are plotted against temperature, where L is the initial length of the pellet in axial direction and dL is its increment. The corresponding shrinkage rates $d(dL/L)/dt$ of the above pellets are shown in Fig. 3.

The onset temperature of shrinkage was determined from shrinkage curves by extrapolating method (as the point at which it deviates from its horizontal path). The onset of sintering was found to marginally shift to higher temperature by increasing the UO_2 content. It can be seen from the Fig. 2 that the onset of the shrinkage occurs at 707 °C for ThO_2-5%UO_2 and 735 °C for ThO_2-10%UO_2 in Ar+5%H_2 atmosphere.
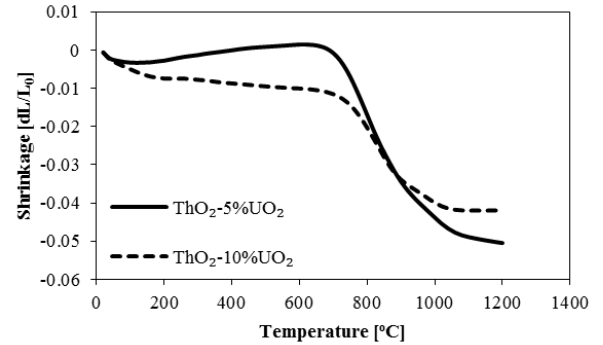

Fig. 2. Shrinkage curves for ThO_2-5%UO_2 and ThO_2-10%UO_2 pellets in Ar-5%H_2. The dL/L_0 values plotted against temperature, where L_0 is the initial length.
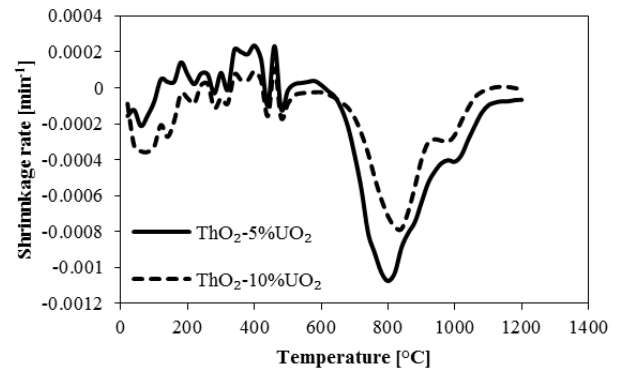

Fig. 3. Shrinkage rate $d(dL/L_0)/dt$ of ThO_2-5%UO_2 and ThO_2-10%UO_2 pellets in Ar-5%H_2 atmosphere plotted against temperature.

Figure 3 shows the shrinkage rate for ThO_2-UO_2 pellets for the different UO_2 content used in this study. From the shrinkage rate curves, it was observed that the maximum shrinkage rates for ThO_2-5%UO_2 and ThO_2-10%UO_2 pellets occur at around 800 °C and 840 °C, respectively. The maximum shrinkage rate shifts to higher temperature with increasing the UO_2 content.

Figure 4 gives the plots of $\log Y' = \log(dY/dt)$ vs. $\log t$ for the ThO_2-5%UO_2 and ThO_2-10%UO_2 pellets at temperatures of 1200 °C, 1100 °C and 1000 °C, as is mentioned in the plots, respectively. The slope of the curves will be $(n-1)$ from the sintering exponent n, which can
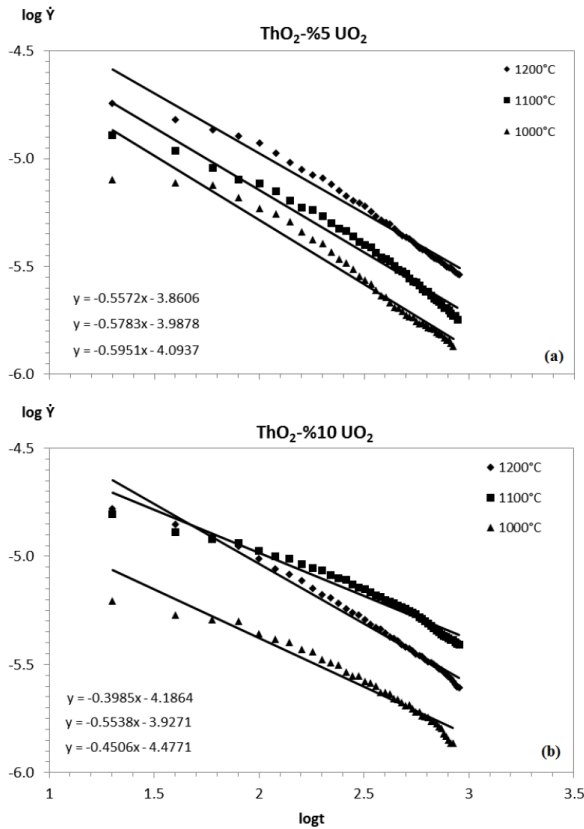
Fig. 4. A plot of $\log Y'$ versus $\log t$ for the pellet (a) ThO$_2$-5%UO$_2$ and (b) ThO$_2$-10%UO$_2$ sintered in Ar+5%H$_2$.

Fig. 5. The Arrhenius plot $\ln D$ versus $1/T$ for (a) ThO$_2$-5%UO$_2$ and (b) ThO$_2$-10%UO$_2$ pellet sintered in Ar+5%H$_2$. The slope of this curve will be Q/R, from which the activation energy Q can be calculated.

be thus evaluated. n is a constant which value depends on the sintering mechanism. The value of n obtained for pellets sintered in Ar+5%H$_2$ is ~ 0.50. The mechanism for the initial stage of sintering was considered to be the volume diffusion. Aybers [18] also specified that volume diffusion controls the first stage of sintering kinetic mechanism for (Th,U)O$_2$. The present study is in compliance with Aybers with respect to the volume diffusion mechanism.

After the determination of parameter n from the straight line of the $\log Y'$–$\log t$ curves, the diffusion coefficient D is going to be calculated using parameter n and Arrhenius constant, $K(T)$. Arrhenius constant is calculated from the intercept of the plot. Finally, the activation energies for sintering pellets are going to be calculated from the slope of the variation of $\log D$ versus $1/T$.

The diffusion coefficients are calculated from the intercepts in Fig. 4 using Eq. 2 and Eq. 3. The values of parameters of the ThO$_2$-5%UO$_2$ and ThO$_2$-10%UO$_2$ powder, used for this calculation, are given in Table I. The $\ln D$ versus $1/T$ plots for ThO$_2$-5%UO$_2$ and ThO$_2$-10%UO$_2$ pellets in Ar+5% H$_2$ atmosphere are shown in Fig. 5.

Finally, the activation energies for the sintered pellets were calculated from the slope of the variation of $\ln D$
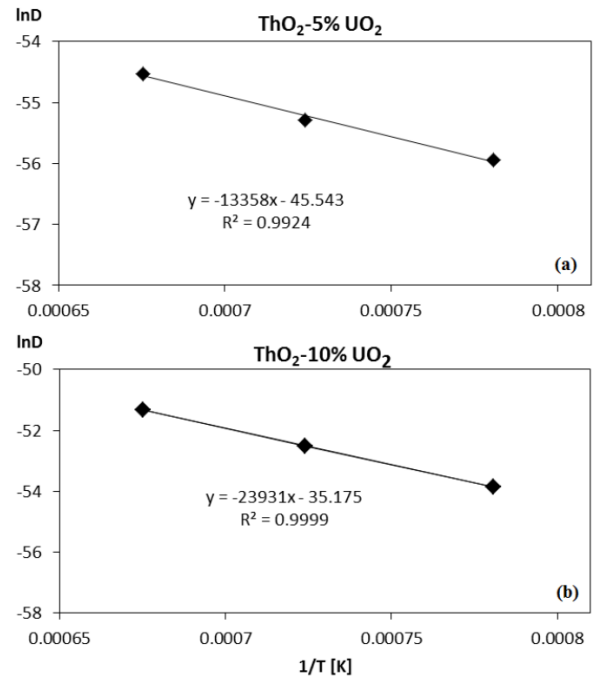
versus $1/T$. The activation energy of sintering for ThO$_2$-5%UO$_2$ and ThO$_2$-10%UO$_2$, determined from dilatometric experiments was found to be 111.58 kJ/mole and 198.96 kJ/mole respectively.

Compared with the conventional powder metallurgy method, the activation energy of (Th,U)O$_2$ pellets present in the study is rather low. Aybers [18] studied the first-stage sintering of ThO$_2$-80%UO$_2$, ThO$_2$-2%0UO$_2$ and ThO$_2$-5%UO$_2$ using a dilatometer. With the aid of shrinkage curves, the apparent activation energy of ThO$_2$-80%UO$_2$ ThO$_2$-2%0UO$_2$ and ThO$_2$-5%UO$_2$ for the initial stages of sintering in reducing atmosphere are calculated to be about 339 kJ/mole, 478.75 kJ/mole and 324 kJ/mole, respectively. Recently, Kutty et al. [19] has estimated activation energy of ThO$_2$-2%U$_3$O$_8$ pellet made by powder metallurgy route using master sintering curve approach, and obtained activation energy of 500 kJ/mole for the above composition.

5. Conclusion

ThO$_2$-5%UO$_2$ and ThO$_2$-%10UO$_2$ pellets have been fabricated by internal gelation technique using nitrates of uranium and thorium as starting material.

The sintering behavior of the ThO$_2$-5%UO$_2$ and ThO$_2$-%10UO$_2$ pellets were studied using a high temperature dilatometer in reducing Ar-5%H$_2$ atmosphere. The activation energies at initial stage of sintering were estimated by applying the sintering-rate equation to isothermal shrinkage data.

The following conclusions were drawn:

- The mechanism for the initial stage of sintering was found to be the volume diffusion for both ThO_2-5%UO_2 and ThO_2-%10UO_2 pellets.

- The onset of sintering was found to marginally shift to higher temperature on increasing the UO_2 content.

- The maximum shrinkage rate shifts to higher temperature by increasing the UO_2 content.

- The shrinkage rate of the ThO_2-5%UO_2 pellet was higher than the ThO_2-%10UO_2 pellet.

- The activation energies for initial stage of sintering were found to be 111.058 kJ/mole and 198.96 kJ/mole for ThO_2-5%UO_2 and ThO_2-%10UO_2 pellets, respectively.

References

[1] W.J. Lackey, J.E. Selle, *Assessment of Gel-Sphere-Pac Fuel for Fast Breeder Reactors*, ORNL-5468, Oak Ridge National Laboratory, Oak Ridge, Tenn., 1978.

[2] N. Kumar, V.P. Rajesh, J.K. Joshi, S.K. Mukerjee, V.N. Vaidya, V. Venugopal, *J. Nucl. Mater.* **359**, 69 (2006).

[3] S. Yamagishi, Y. Takahashi, *J. Nucl. Mater.* **217**, 127 (1994).

[4] E. Zimmer, C. Ganguly, J. Borchardt, H. Langan, *J. Nucl. Mater.* **152**, 169 (1988).

[5] R.B. Matthews, P.E. Hart, *J. Nucl. Mater.* **92**, 207 (1980).

[6] Hj. Matzke, *J. Chem. Soc. Faraday Trans.* **86**, 1243 (1990).

[7] C.R.A. Catlow, *J. Chem. Soc. Faraday Trans. 2* **83**, 1065 (1987).

[8] R.M. German, C.A. Labombard, *Int. J. Powder Metall. Powder Technol.* **18**, 147 (1982).

[9] Hj. Matzke, *Nonstoichiometric Oxides,* Ed. by T. Sorensen, Academic Press, New York, 1981.

[10] T.R.G. Kutty, P.V. Hegde, K.B. Khan, S. Majumdar, D.S.C. Purushotham, *J. Nucl. Mater.* **282**, 54 (2000).

[11] M.T. Aybers, *J. Nucl. Mater.* **210**, 73 (1994).

[12] M.T. Aybers, *J. Nucl. Mater.* **226**, 27 (1995).

[13] Y. Altas, M. Eral, H. Tel, *J. Nucl.Mater.* **249**, 46 (1997).

[14] T.R.G. Kutty, P.V. Hedge, K.B. Khan, T. Jarvis, A.K. Sengupta, S. Majumdar, H.S. Kamath, *J. Nucl. Mater.* **335**, 462 (2004).

[15] N. Hingant, N. Clavier, N. Dacheux, S. Hubert, N. Barré, R. Podor, L. Aranda, *Powder Technol.* **208**, 454 (2011).

[16] M.M. El-Sayed Ali, PhD. Thesis, *Etude Du Stade Initiale De Frittage Des Oxydes D'Actinides: UO_2, PuO_2 et De Leurs Mélanges*, Université Pierre et Marie Curie, Paris, 1979.

[17] H.G. Riella, L.G. Martinez, K. Imakuma, *J. Nucl. Mat.* **153**, 71 (1988).

[18] M.T.Aybers, PhD. Thesis, *UO_2, ThO_2ve $(Th,U)O_2$ Peletlerinin Birinci Safha Sinterleme Kinetiğinin İncelenmesi*, Istanbul Technical University, Istanbul, 1989.

[19] T.R.G. Kutty, K.B. Khan, P.V. Hegde, A.K. Sengupta, S. Majumdar, H.S. Kamath, *Sci. of Sinter.* **35**, 125 (2003).